

Doped bilayer antiferromagnets: Hole dynamics on both sides of a magnetic ordering transition

Matthias Vojta^(a) and Klaus W. Becker^(b)

^(a) *Department of Physics and Applied Physics, Yale University, New Haven, CT 06520, USA*

^(b) *Institut für Theoretische Physik, Technische Universität Dresden, D-01062 Dresden, Germany*

The two-layer square lattice quantum antiferromagnet with spins $\frac{1}{2}$ shows a magnetic order-disorder transition at a critical ratio of the interplane to intraplane couplings. We investigate the dynamics of a single hole in a bilayer antiferromagnet described by a $t-J$ Hamiltonian. To model the spin background we propose a ground-state wave function for the undoped system which covers both magnetic phases and includes transverse as well as longitudinal spin fluctuations. The photoemission spectrum is calculated using the spin-polaron picture for the whole range of the ratio of the magnetic couplings. This allows for the study of the hole dynamics of both sides of the magnetic order-disorder transition. For small interplane coupling we find a quasiparticle with properties known from the single-layer antiferromagnet, e.g., the dispersion minimum is at $(\pm\pi/2, \pm\pi/2)$. For large interplane coupling the hole dispersion is similar to that of a free fermion (with reduced bandwidth). The cross-over between these two scenarios occurs inside the antiferromagnetic phase which indicates that the hole dynamics is governed by the local environment of the hole.

I. INTRODUCTION

Since the discovery of high-temperature superconductivity, doped antiferromagnets (AF) have been studied intensively. It is widely accepted that many properties of the superconducting cuprates are determined by the hole-doped CuO_2 planes. A number of experiments¹ indicate that the cuprates are near a quantum-critical point of antiferromagnetic instability: The undoped materials are known to be antiferromagnetic Mott-Hubbard insulators, whereas hole doping destroys the antiferromagnetic long-range order (LRO) and leads to superconductivity. The investigation of the interplay between long-range magnetic order and quantum disorder is therefore of great theoretical interest.

A model system which shows a quantum transition between an ordered and a disordered magnetic phase is the $S = \frac{1}{2}$ bilayer antiferromagnet²⁻⁹. Here each of the two planes is composed of a nearest-neighbor Heisenberg model with coupling constant J_{\parallel} . The spins of corresponding sites of each layer are coupled antiferromagnetically with a coupling constant J_{\perp} . In the limit of small J_{\perp}/J_{\parallel} the model describes two weakly coupled AF planes. At $T = 0$ this system possesses AF long-range order and gapless Goldstone excitations. In the opposite case of large J_{\perp}/J_{\parallel} , pairs of spins interacting via J_{\perp} form spin singlets being weakly coupled by J_{\parallel} . Then the spin excitations are gapped triplet modes, there is no magnetic LRO. At a critical ratio $(J_{\perp}/J_{\parallel})_c$ a quantum transition between the two phases occurs which is believed to be of the $O(3)$ universality class²⁻⁵. The bilayer antiferromagnet has been studied by a number of numerical and analytical techniques. Quantum Monte Carlo calculations^{3,4} and series expansions⁶ yield an order-disorder transition point of $(J_{\perp}/J_{\parallel})_c \sim 2.5$. A

similar result has also been obtained analytically using a diagrammatic approach to account for the hard-core interaction between triplet excitations⁷. Bond-operator mean-field theory has recently been applied to the bilayer Heisenberg AF¹⁰ and gives a transition point of $(J_{\perp}/J_{\parallel})_c \sim 2.3$. Note that Schwinger boson mean-field theory⁹ predicts a very large value of $(J_{\perp}/J_{\parallel})_c \sim 4.5$, and also self-consistent spin-wave theory^{2,8}, which yields $(J_{\perp}/J_{\parallel})_c \sim 4.3$, fails to reproduce the numerical results. Chubukov and Morr² have pointed out that this discrepancy is due to the neglect of longitudinal spin fluctuations in the conventional spin-wave approach.

In this paper we discuss the bilayer antiferromagnet at zero temperature with hole doping as an additional degree of freedom. We consider the standard $t-J$ model on a bilayer square lattice consisting of N sites per plane, so the total number of lattice sites is $2N$. Each pair of corresponding sites in different planes is considered to form a rung, so we have N rungs. More precisely, the Hamiltonian reads

$$\begin{aligned}
 H = & -t_{\perp} \sum_{i\sigma} (\hat{c}_{i1,\sigma}^{\dagger} \hat{c}_{i2,\sigma} + H.c.) \\
 & -t_{\parallel} \sum_{\langle ij \rangle m \sigma} (\hat{c}_{im,\sigma}^{\dagger} \hat{c}_{jm,\sigma} + H.c.) \\
 & + J_{\perp} \sum_i (\mathbf{S}_{i1} \cdot \mathbf{S}_{i2} - \frac{n_{i1} n_{i2}}{4}) \\
 & + J_{\parallel} \sum_{\langle ij \rangle m} (\mathbf{S}_{im} \cdot \mathbf{S}_{jm} - \frac{n_{im} n_{jm}}{4}). \quad (1)
 \end{aligned}$$

Here and in the following i and j denote *rungs* of the bilayer lattice, $\langle ij \rangle$ denotes a summation over all pairs of nearest-neighbor rungs. $m = 1, 2$ is the plane index, so im denotes a lattice site. \mathbf{S}_{im} is the electronic spin operator and n_{im} the electron number operator at site

im. The electron operators $\hat{c}_{im,\sigma}^\dagger$ exclude double occupancies, $\hat{c}_{im,\sigma}^\dagger = c_{im,\sigma}^\dagger(1 - n_{im,-\sigma})$. We choose the z -axis along the direction of the rungs, i.e., perpendicular to the planes.

First we want to comment the zero-temperature phase diagram of the doped bilayer $t - J$ model which has to our knowledge not been systematically studied up to now. The following non-thermal control parameters can be considered: the ratio J_\perp/J_\parallel , the doping level δ , and the relative hopping strength t/J . The doped single-layer antiferromagnet is known to exhibit a strong dependence of magnetic properties on the hole concentration δ . With increasing hole concentration the staggered magnetization decreases and vanishes at a critical hole concentration δ_c of a few percent where the system becomes paramagnetic^{11–14}. (This is consistent with experiments on high- T_c superconductors^{11,12}.) On the other hand, in the undoped limit a large interplane coupling J_\perp also destroys the antiferromagnetic LRO as discussed above. Thus it is likely that the system shows (i) AF LRO accompanied by spontaneous symmetry breaking and the existence of massless Goldstone modes in the region of very small doping and small J_\perp . Otherwise it is paramagnetic; here one has to distinguish between (ii) a spin-gapped phase which occurs at small δ , small hopping t_\parallel , and large interplane coupling, and (iii) a gapless phase at larger doping and small interplane coupling. The gapped phase (ii) is dominated by interplane singlet pairs (incompressible spin fluid) whereas the gapless phase (iii) shows only weak interplane coupling and behaves mainly like a single layer system at $\delta > \delta_c$ (compressible spin fluid). (Issues like pseudogap features and transport properties will not be addressed here.) In the present work we restrict ourselves to the zero-doping limit (one hole). So the magnetic (bulk) properties will not be affected by the doped hole, i.e., we probe the transition between the antiferromagnetic (i) and the gapped (incompressible) paramagnetic phase (ii).

The dynamical properties of holes in high- T_c superconductors have been subject to a lot of experimental and theoretical work. Angle-resolved photoemission (ARPES) experiments at zero¹⁵ or small doping^{16,17} indicate a quasiparticle band with a small bandwidth providing evidence for strong electronic correlations in the high- T_c compounds. A large number of numerical and analytical studies reveal that a single hole in an AF spin background has non-trivial properties: The spectral function consists of a pronounced coherent peak at the bottom of the spectrum and a incoherent background at higher energies. The coherent peak can be associated with the motion of a dressed hole, i.e., a hole surrounded by spin defects ("spin polaron")^{11,12,18–23}. The hole motion in bilayer antiferromagnets has been studied in a few papers and only for a small parameter range: Using self-consistent Born approximation (SCBA) it has been shown²⁴ that small interplane coupling only weakly affects the hole properties. Exact diagonalization studies²⁵

have indicated a larger effect of the interplane coupling at finite doping. However, the system sizes accessible to numerical methods (2×8 in Ref. 25) do not allow for the study of small hole densities and arbitrary momenta.

In this paper we prefer an analytical approach to the one-hole problem which is based on the picture of the spin-bag quasiparticle (QP) or magnetic polaron^{18–23}. The magnetic background for the hole motion will be modelled within a modified bond-operator representation of the spins on each rung. In the ordered phase one type of triplet bosons condenses which will be included in the modified basis operators. So our excitation operators continuously interpolate between the triplet excitations of a singlet product state and the transverse and longitudinal excitations of a Néel-ordered state. The deviations of the spin background caused by the hole motion are described by a set of path operators^{18,19,22,23}. The one-hole spectral function will be evaluated using a cumulant version^{26,27} of Mori-Zwanzig projection technique²⁸.

The paper is organized as follows: In Sec. II we propose a ground-state wave function for the undoped bilayer antiferromagnet. In Sec. III we develop the Hamiltonian for the doped system in this new operator representation and discuss the various hole motion processes. Sec. IV focuses on the motion of a single hole in an otherwise half-filled bilayer antiferromagnet. The one-hole spectral function for this case corresponds directly to the result of an ARPES experiment on an undoped system. After a brief sketch of the projection technique we investigate the spectral properties in dependence of the magnetic background, especially when crossing the phase boundary between gapped paramagnet and antiferromagnet. The results show that the character of the one-hole spectrum is mainly determined by the local spin environment of the hole whereas the spectrum changes only weakly when crossing the order-disorder transition. A conclusion will close the paper.

II. UNDOPED BILAYER ANTIFERROMAGNET

To begin with, we consider the case of half-filling. Using bond operators we derive a wave function which describes the ground states in both the quantum disordered phase (at large J_\perp) and the Néel phase (at small J_\perp). The wave function will be constructed within a cumulant formalism^{26,29}. It bases on an expansion around a product of rung states which are singlets in the disordered phase and sums of singlets and z -type triplets in the ordered phase. This wave function will be used in Sec. IV as "magnetic background" to calculate dynamical properties of a single hole.

A. Rung basis and Hamiltonian

In the limit of vanishing intraplane coupling, $J_{\parallel}/J_{\perp} \rightarrow 0$, pairs of spins on each rung form a singlet ground state. The excitations are localized triplets with an energy gap J_{\perp} . Switching on J_{\parallel} leads to an interaction of triplets

$$\begin{aligned} s_i^{\dagger}|0\rangle &= \frac{1}{\sqrt{2}}(\hat{c}_{i1,\uparrow}^{\dagger}\hat{c}_{i2,\downarrow}^{\dagger} - \hat{c}_{i1,\downarrow}^{\dagger}\hat{c}_{i2,\uparrow}^{\dagger})|0\rangle = \frac{1}{\sqrt{2}}(|\uparrow\downarrow\rangle - |\downarrow\uparrow\rangle), \\ t_{ix}^{\dagger}|0\rangle &= \frac{-1}{\sqrt{2}}(\hat{c}_{i1,\uparrow}^{\dagger}\hat{c}_{i2,\uparrow}^{\dagger} - \hat{c}_{i1,\downarrow}^{\dagger}\hat{c}_{i2,\downarrow}^{\dagger})|0\rangle = \frac{-1}{\sqrt{2}}(|\uparrow\uparrow\rangle - |\downarrow\downarrow\rangle), \\ t_{iy}^{\dagger}|0\rangle &= \frac{i}{\sqrt{2}}(\hat{c}_{i1,\uparrow}^{\dagger}\hat{c}_{i2,\uparrow}^{\dagger} + \hat{c}_{i1,\downarrow}^{\dagger}\hat{c}_{i2,\downarrow}^{\dagger})|0\rangle = \frac{i}{\sqrt{2}}(|\uparrow\uparrow\rangle + |\downarrow\downarrow\rangle), \\ t_{iz}^{\dagger}|0\rangle &= \frac{1}{\sqrt{2}}(\hat{c}_{i1,\uparrow}^{\dagger}\hat{c}_{i2,\downarrow}^{\dagger} + \hat{c}_{i1,\downarrow}^{\dagger}\hat{c}_{i2,\uparrow}^{\dagger})|0\rangle = \frac{1}{\sqrt{2}}(|\uparrow\downarrow\rangle + |\downarrow\uparrow\rangle). \end{aligned} \quad (2)$$

Then the following representation holds³⁰:

$$S_{i1,2}^{\alpha} = \frac{1}{2}(\pm s_i^{\dagger} t_{i\alpha} \pm t_{i\alpha}^{\dagger} s_i - i\epsilon_{\alpha\beta\gamma} t_{i\beta}^{\dagger} t_{i\gamma}). \quad (3)$$

The algebra of the operators $\{s_i, t_{ix}, t_{iy}, t_{iz}\}$ has to be specified to reproduce the correct algebra for the spin operators. Here bond operators satisfying the usual bosonic commutation relations will be chosen³⁰. In order to ensure that the physical states are either singlets or triplets one has to impose the condition:

$$s_i^{\dagger} s_i + \sum_{\alpha} t_{i\alpha}^{\dagger} t_{i\alpha} = 1. \quad (4)$$

The singlet product ground state for $J_{\parallel}/J_{\perp} \rightarrow 0$ can be written as

$$|\phi_0\rangle = \prod_i s_i^{\dagger}|0\rangle. \quad (5)$$

We can now substitute the operator representation (3) into the Heisenberg Hamiltonian for the bilayer and obtain the following Hamiltonian $H = H_0 + H_1$ in the bond (rung) operator representation^{31,32}:

$$\begin{aligned} H_0 &= J_{\perp} \sum_{i\alpha} t_{i\alpha}^{\dagger} t_{i\alpha}, \\ H_1 &= \frac{J_{\parallel}}{2} \sum_{\langle ij \rangle \alpha} (t_{i\alpha}^{\dagger} t_{j\alpha}^{\dagger} s_j s_i + H.c.) \\ &+ \frac{J_{\parallel}}{2} \sum_{\langle ij \rangle \alpha} (t_{i\alpha}^{\dagger} s_j^{\dagger} t_{j\alpha} s_i + H.c.) \\ &- \frac{J_{\parallel}}{2} \sum_{\langle ij \rangle \alpha\beta} (t_{i\alpha}^{\dagger} t_{j\alpha}^{\dagger} t_{j\beta} t_{i\beta} - t_{i\alpha}^{\dagger} t_{j\beta}^{\dagger} t_{j\alpha} t_{i\beta}). \end{aligned} \quad (6)$$

The sum $\langle ij \rangle$ runs over pairs of neighboring rungs of the lattice. The ground state of H_0 is given by the product state $|\phi_0\rangle$ defined in eq. (5).

Approaching the quantum critical point the triplet excitations will become gapless at momentum (π, π) , see

on neighboring rungs and to a dispersion of the triplet excitations. To describe this dimerized phase we employ a bond operator representation³⁰ for the spins per rung. For each rung i containing two $S = 1/2$ spins $\mathbf{S}_{i1}, \mathbf{S}_{i2}$ we introduce operators for creation of a singlet and three triplet states out of the vacuum $|0\rangle$:

e.g. Refs. 2,6. The magnetic quantum phase transition to an antiferromagnetically ordered state includes spontaneous symmetry breaking and can be described via the condensation of triplet bosons in one particular direction (which has to be induced by an infinitesimal staggered field). Neglecting fluctuations a symmetry-broken state with a condensate of z -type triplet bosons can be written as

$$\begin{aligned} |\tilde{\phi}_0\rangle &\sim \\ \exp(\lambda \sum_i e^{i\mathbf{Q}\mathbf{R}_i} t_{iz}^{\dagger}) |\phi_0\rangle &= \prod_i (s_i^{\dagger} + \lambda e^{i\mathbf{Q}\mathbf{R}_i} t_{iz}^{\dagger}) |0\rangle \end{aligned} \quad (7)$$

where the spontaneous staggered magnetization points in z -direction. The exponential term accounts for boson condensation, the condensation amplitude is given by λ . $\lambda = 0$ means rotational symmetry in spin space (then $|\tilde{\phi}_0\rangle = |\phi_0\rangle$), $\lambda \neq 0$ breaks this symmetry. $\lambda = \pm 1$ transforms the singlet product state $|\phi_0\rangle$ into a Néel state. $\mathbf{Q} = (\pi, \pi)$ is the AF ordering wave vector.

The basic idea for a proper description of the excitations of the product state $|\phi_0\rangle$ (7) is now to transform the basis states on each rung. We replace the basis operators s_i for singlets and t_{iz} for z -triplets by

$$\begin{aligned} \tilde{s}_i &= \frac{1}{\sqrt{1+\lambda^2}} (s_i + \lambda e^{i\mathbf{Q}\mathbf{R}_i} t_{iz}), \\ \tilde{z}_i &= \frac{1}{\sqrt{1+\lambda^2}} (-\lambda e^{i\mathbf{Q}\mathbf{R}_i} s_i + t_{iz}). \end{aligned} \quad (8)$$

The new basis per rung consists of the operators $\{\tilde{s}_i, \tilde{z}_i, t_{ix}, t_{iy}\}$ which still satisfy bosonic commutation relations. For $\lambda = 0$ this basis reproduces the usual bond-boson basis. For non-zero λ the state $\tilde{s}_i^{\dagger}|0\rangle$ interpolates between the rung singlet and a (local) Néel state, the state $\tilde{z}_i^{\dagger}|0\rangle$ is orthogonal to $\tilde{s}_i^{\dagger}|0\rangle$. The product state $|\tilde{\phi}_0\rangle$ (7) can now be written as

$$|\tilde{\phi}_0\rangle = \prod_i \tilde{s}_i^{\dagger}|0\rangle. \quad (9)$$

For $|\lambda| = 1$ this state is an antiferromagnetic Néel state. Its excitations are given by $t_{ix}^\dagger \tilde{s}_i$, $t_{iy}^\dagger \tilde{s}_i$, and $\tilde{z}_i^\dagger \tilde{s}_i$. Here, $(t_{ix}^\dagger \pm it_{iy}^\dagger) \tilde{s}_i$ create one spin flip in one of the planes and can be regarded as transverse spin fluctuations. The operator $\tilde{z}_i^\dagger \tilde{s}_i$ flips both spins on one rung which can be interpreted as longitudinal spin fluctuation. The basis parameter λ has to be determined separately which will be discussed in the next subsection. Below it is shown that in the ordered phase λ varies continuously between

$$\begin{aligned}
\tilde{H}_0 &= J_\perp \sum_i \left(t_{ix}^\dagger t_{ix} + t_{iy}^\dagger t_{iy} + \frac{1}{1+\lambda^2} \left(\tilde{z}_i^\dagger \tilde{z}_i + \lambda^2 \tilde{s}_i^\dagger \tilde{s}_i \right) \right), \\
\tilde{H}_1 &= J_\perp \sum_i \frac{\lambda}{1+\lambda^2} e^{i\mathbf{QR}_i} (\tilde{z}_i^\dagger \tilde{s}_i + \tilde{s}_i^\dagger \tilde{z}_i) \\
&+ \frac{J_\parallel}{2} \sum_{\langle i \in A, j \in B \rangle} \left((t_{ix}^\dagger t_{jx}^\dagger + t_{iy}^\dagger t_{jy}^\dagger) (\tilde{s}_i \tilde{s}_j - \tilde{z}_i \tilde{z}_j) + H.c. \right) \\
&+ \frac{J_\parallel}{2} \sum_{\langle i \in A, j \in B \rangle} \left(t_{ix}^\dagger t_{jx}^\dagger t_{iy} t_{jy} - t_{ix}^\dagger t_{jy}^\dagger t_{iy} t_{jx} + H.c. \right) \\
&+ \frac{J_\parallel}{2(1+\lambda^2)} \sum_{\langle i \in A, j \in B \rangle} \left(t_{ix}^\dagger \tilde{s}_j^\dagger \left((1-\lambda^2) \tilde{s}_i t_{jx} - 2\lambda \tilde{z}_i t_{jx} \right) + t_{iy}^\dagger \tilde{s}_j^\dagger \left((1-\lambda^2) \tilde{s}_i t_{jy} - 2\lambda \tilde{z}_i t_{jy} \right) + H.c. \right) \\
&+ \frac{J_\parallel}{2(1+\lambda^2)} \sum_{\langle i \in A, j \in B \rangle} \left(t_{ix}^\dagger \tilde{z}_j^\dagger \left((1-\lambda^2) \tilde{z}_i t_{jx} + 2\lambda \tilde{s}_i t_{jx} \right) + t_{iy}^\dagger \tilde{z}_j^\dagger \left((1-\lambda^2) \tilde{z}_i t_{jy} + 2\lambda \tilde{s}_i t_{jy} \right) + H.c. \right) \\
&+ \frac{J_\parallel}{2(1+\lambda^2)^2} \sum_{\langle i \in A, j \in B \rangle} 4\lambda^2 \left(-\tilde{s}_i^\dagger \tilde{s}_j^\dagger \tilde{s}_j \tilde{s}_i - \tilde{z}_i^\dagger \tilde{z}_j^\dagger \tilde{z}_j \tilde{z}_i + \tilde{z}_i^\dagger \tilde{s}_j^\dagger \tilde{s}_j \tilde{z}_i + \tilde{s}_i^\dagger \tilde{z}_j^\dagger \tilde{z}_j \tilde{s}_i \right) \\
&+ \frac{J_\parallel}{2(1+\lambda^2)^2} \sum_{\langle i \in A, j \in B \rangle} \left((1-\lambda^2)^2 (\tilde{z}_i^\dagger \tilde{z}_j^\dagger \tilde{s}_i \tilde{s}_j + \tilde{z}_i^\dagger \tilde{s}_j^\dagger \tilde{s}_i \tilde{z}_j) + 2\lambda(1-\lambda^2) (\tilde{s}_i^\dagger \tilde{z}_j^\dagger - \tilde{z}_i^\dagger \tilde{s}_j^\dagger) \tilde{s}_i \tilde{s}_j + H.c. \right). \quad (10)
\end{aligned}$$

A and B denote the sublattices of the square lattice, i.e., $e^{i\mathbf{QR}_i} = \pm 1$ for $i \in A$ or B , respectively. For $\lambda = 0$ the Hamiltonian (10) is identical to (6) derived with the usual bond operators. For $|\lambda| \leq 1$ the ground state of \tilde{H}_0 defined in (10) is given by the modified product state $|\tilde{\phi}_0\rangle$ (9). It can be seen that \tilde{H}_1 in (10) contains creation, hopping, and conversion terms of the three types of excitations $\{\tilde{z}_i, t_{ix}, t_{iy}\}$. Contrary to the Hamiltonian H_1 in (6) where the triplet excitations can only occur in pairs, here also single \tilde{z} -type excitations can be created and destroyed, e.g., by $J_\perp (\tilde{z}_i^\dagger \tilde{s}_i + \tilde{s}_i^\dagger \tilde{z}_i)$. The effect of these terms is directly related to the basis parameter λ and will be used to determine its value. Furthermore it can be seen that all terms creating \tilde{z} -type excitations out of $|\tilde{\phi}_0\rangle$ vanish for $J_\perp = 0, |\lambda| = 1$. This means that the ground state in the limit of vanishing interplane coupling J_\perp does not contain single longitudinal spin fluctuations. They will become, however, important for describing the destruction of the antiferromagnetism with increasing J_\perp .

Note that \tilde{z} -type bosons formally occur together with transverse fluctuations even at $J_\perp = 0, |\lambda| = 1$. This happens if a transverse fluctuation created by J_\parallel hits

$\lambda = 1$ for $J_\perp = 0$ and $\lambda = 0$ at the transition to the disordered phase. Note that the idea of a condensate for one type of bosons has also been employed by Chubukov and Morr² who applied a modified version of non-linear spin-wave theory to the problem of the undoped bilayer antiferromagnet.

Using (8) we can reformulate the Hamiltonian for the (undoped) bilayer Heisenberg model in terms of the new basis operators $\{\tilde{s}_i, \tilde{z}_i, t_{ix}, t_{iy}\}$. Note that the splitting of the Hamiltonian is different from (6).

a second transverse fluctuation being already present at the same rung, in other words, if spins on corresponding sites in each of the planes are flipped independently by J_\parallel . These processes have to be included in an exact treatment of the ground-state wave function; within the approximation of independent bosons (which will be described in Sec. II C) they are neglected.

B. Approximation for the ground state

To obtain an approximation for the ground-state wave function we adopt a cumulant approach²⁶ which has been successfully applied to a variety of strongly correlated systems. One starts from a splitting of the Hamiltonian into $H = H_0 + H_1$ where eigenstates and eigenvalues of H_0 are known. The ground state $|\psi_0\rangle$ of H can be constructed from the unperturbed ground state $|\phi_0\rangle$ of H_0 by application of a so-called wave operator Ω which contains the effect of H_1 . It has been shown²⁹ that Ω can be written in an exponential form, $\Omega = e^S$, where S introduces fluctuations into $|\phi_0\rangle$. The ground-state energy

E is calculated²⁶ according to $E = \langle \phi_0 | H \Omega | \phi_0 \rangle^c$ where $\langle \phi_0 | \dots | \phi_0 \rangle^c$ denotes a cumulant expectation value with respect to $|\phi_0\rangle$.

For the disordered phase of the system it is suitable to start from the singlet product state $|\phi_0\rangle$ given in eq. (5) and to include fluctuations in form of pairs of triplet excitations. An appropriate ansatz for the wave function is

$$|\psi_0\rangle = \Omega |\phi_0\rangle = \exp\left(\sum_{ij\alpha} \mu_{ij\alpha} t_{i\alpha}^\dagger t_{j\alpha}^\dagger s_j s_i + \sum_n \beta_n S_n\right) |\phi_0\rangle. \quad (11)$$

The first term in the exponential contains pairs of triplets (with arbitrary distance $\mathbf{R}_i - \mathbf{R}_j$). The operators S_n in the second term represent higher-order fluctuations, e.g., four-triplet operators. They will be used in Sec. IV. For the determination of the coefficients $\mu_{ij\alpha}$ and β_n the cumulant method provides a set of non-linear equations²⁹,

$$\begin{aligned} 0 &= \langle \phi_0 | (s_i^\dagger s_j^\dagger t_{j\alpha} t_{i\alpha}) \cdot H \Omega | \phi_0 \rangle^c, \\ 0 &= \langle \phi_0 | S_n^\dagger H \Omega | \phi_0 \rangle^c. \end{aligned} \quad (12)$$

$$|\psi_0\rangle = \Omega |\tilde{\phi}_0\rangle = \exp\left(\sum_{ij} \mu_{ij} (t_{ix}^\dagger t_{jx}^\dagger + t_{iy}^\dagger t_{jy}^\dagger) \tilde{s}_j \tilde{s}_i + \sum_{ij} \nu_{ij} \tilde{z}_i^\dagger \tilde{z}_j^\dagger \tilde{s}_j \tilde{s}_i + \sum_n \beta_n S_n\right) |\tilde{\phi}_0\rangle. \quad (13)$$

The operators S_n again contain higher-order fluctuations and will be discussed later. The parameters μ_{ij} , ν_{ij} , and β_n have to be determined in analogy to (12) by the equations

$$\begin{aligned} 0 &= \langle \tilde{\phi}_0 | (\tilde{s}_i^\dagger \tilde{s}_j^\dagger t_{jx} t_{ix}) \cdot H \Omega | \tilde{\phi}_0 \rangle^c, \\ 0 &= \langle \tilde{\phi}_0 | (\tilde{s}_i^\dagger \tilde{s}_j^\dagger \tilde{z}_j \tilde{z}_i) \cdot H \Omega | \tilde{\phi}_0 \rangle^c, \\ 0 &= \langle \tilde{\phi}_0 | S_n^\dagger H \Omega | \tilde{\phi}_0 \rangle^c \end{aligned} \quad (14)$$

which again reduce to (12) in the case of $\lambda = 0$. For $\lambda = 0$ we expect the transverse and longitudinal fluctuations to become equivalent, $\mu_{ij} = \nu_{ij}$. For $|\lambda| = 1$ the amplitude of the longitudinal fluctuations in the ground state vanishes, $\nu_{ij} = 0$, if one neglects higher-order processes in J_{\parallel} as noted above. Note that Ω in (13) does not contain operators for the creation of single \tilde{z} -type excitations ($\tilde{z}_i^\dagger \tilde{s}_i$) although such operators are present in the Hamiltonian (10). The reason is that such operators change the density of the condensate of the z triplet bosons and refer to the same degree of freedom as the parameter λ in the product state $|\phi_0\rangle$. The aim here is, however, to describe the condensation of the z -type bosons completely via the introduction of λ and the transformed basis states. In this way Ω contains only multi-spin fluctuations.

Now we discuss the parameter λ which is expected to be zero throughout the disordered phase and to vary continuously from 0 to 1 with decreasing J_{\perp} in the ordered phase. Within the cumulant method λ can be determined consistently using the identity

The dot \cdot indicates that the quantity inside (...) has to be treated as a single entity in the cumulant formation. The equations (12) are derived from the requirement that $\Omega|\phi_0\rangle$ is an eigenstate of H . From symmetry it follows that the coefficients $\mu_{ij\alpha} = \mu_{ij}$ only depend on the difference vector $\mathbf{R}_i - \mathbf{R}_j$ (but not on α). So the state $|\psi_0\rangle$ obeys rotational invariance in spin space. When evaluating the terms in (12) the exponential series terminates after a few terms since the exponent contains only operators which create (but not destroy) fluctuations. The resulting non-linear coupled equations for μ_{ij} can be partially decoupled by a Fourier transformation to momentum space. The remaining set of equations has to be solved self-consistently.

For the ordered phase the treatment is similar, however, one has to take care of the broken rotational symmetry. Starting point is the product wave function $|\tilde{\phi}_0\rangle$ (9). In the operator Ω we now explicitly distinguish between pairs of transverse ($t_{ix}^\dagger t_{jx}^\dagger, t_{iy}^\dagger t_{jy}^\dagger$) and longitudinal ($\tilde{z}_i^\dagger \tilde{z}_j^\dagger$) fluctuations:

$$0 = \langle \tilde{\phi}_0 | (\tilde{s}_i^\dagger \tilde{z}_i) \cdot H \Omega | \tilde{\phi}_0 \rangle^c. \quad (15)$$

This can be understood as the condition that Ω contains **no** additional term like $\sum_i \tilde{z}_i^\dagger \tilde{s}_i$ in the exponential, i.e., the boson condensation is fully accounted for by the transformed basis state $|\tilde{\phi}_0\rangle$. Within the cumulant formalism this can be seen from the equality

$$\begin{aligned} \Omega |\tilde{\phi}_0\rangle^c &= \Omega |e^{\lambda t_{\mathbf{Q}z}^\dagger} \phi_0\rangle^c = \Omega |e^{\lambda t_{\mathbf{Q}z}^\dagger} \phi_0\rangle^c, \\ t_{\mathbf{Q}z} &= \sum_i e^{i\mathbf{Q}\mathbf{R}_i} t_{iz}. \end{aligned} \quad (16)$$

Here we have used the fact that a cumulant expectation value does not change when the operator $e^{\lambda t_{\mathbf{Q}z}^\dagger}$ is subject to cumulant ordering instead of being applied directly to the wave function $|\phi_0\rangle$ (see Ref. 33). The operator $\Omega e^{\lambda t_{\mathbf{Q}z}^\dagger}$ can be interpreted as new wave operator (applied to $|\phi_0\rangle$). It now contains the additional parameter λ which has to be determined from $0 = \langle \phi_0 | (\tilde{s}_i^\dagger \tilde{z}_i) \cdot H \Omega | \phi_0 \rangle^c$ which is equivalent to eq. (15).

C. Ground-state properties

If we restrict the fluctuation operators in the exponential of Ω to excitation pairs as described above (i.e. neglect further operators S_n) and take fully into account the constraint (4), we find a critical coupling of

$(J_{\perp}/J_{\parallel})_c \sim 3.2$ for the order-disorder transition. At this level of approximation the magnetization in the limit of decoupled planes ($J_{\perp} \rightarrow 0$) is around 86 % of its classical value being larger than predicted by Monte-Carlo and spin-wave calculations. The described approximation can be systematically improved by including higher-order fluctuations. This behavior is also known from calculations within the coupled-cluster method for the Heisenberg model³⁴. It can be shown that in the limit of an infinite set of operators the cumulant method yields exact results. For instance, if we include two additional operators S_n with three and four fluctuations on adjacent sites into the operator Ω (13) the transition point shifts to $(J_{\perp}/J_{\parallel})_c \sim 2.9$. However, the analytical and numerical effort to set-up and solve the non-linear equations equivalent to (12,14) increases drastically with including higher-order fluctuations.

The solution of the non-linear equations (12,14) shows that the absolute values of all coefficients in Ω are small compared to 1. In the disordered phase the maximum is taken by $\mu_{10} \sim 0.07$ (the coefficient for nearest-neighbor triplet pairs) at the point of the phase transition. In the ordered phase the maximum is at $J_{\perp} = 0$ with $\mu_{10} \sim 0.14$. With increasing distance between the triplets the values decay fastly; higher-order fluctuations acquire a coefficient being one or more orders smaller in magnitude. The fact that the coefficients are small is equivalent to the statement that the total triplet density even at the transition point is small (~ 0.1), see Ref. 7.

In Fig. 1 we show results for the ground-state energy E and the staggered magnetization M for the approximation using triplet pairs only as described above and for the spin-wave approach (see below). The data are compared with recent series expansions from Ref. 6. It can be seen that all approximations well describe the behavior of the magnetization which first increases with increasing J_{\perp} and then drops to zero at the critical coupling.

$$\begin{aligned}
H^{(sw)} = & \frac{1}{(1+\lambda^2)^2} \sum_{\mathbf{q}} (t_{\mathbf{q}x}^{\dagger} t_{\mathbf{q}x} + t_{\mathbf{q}y}^{\dagger} t_{\mathbf{q}y}) ((1+\lambda^2)J_{\perp} + 8\lambda^2 J_{\parallel} + 2\gamma_{\mathbf{q}}(1-\lambda^4)J_{\parallel}) \\
& + \frac{1}{(1+\lambda^2)^2} \sum_{\mathbf{q}} \tilde{z}_{\mathbf{q}}^{\dagger} \tilde{z}_{\mathbf{q}} ((1-\lambda^4)J_{\perp} + 16\lambda^2 J_{\parallel} + 2\gamma_{\mathbf{q}}(1-\lambda^2)^2 J_{\parallel}) \\
& + J_{\parallel} \sum_{\mathbf{q}} \gamma_{\mathbf{q}} (t_{\mathbf{q}x}^{\dagger} t_{-\mathbf{q}x}^{\dagger} + t_{\mathbf{q}y}^{\dagger} t_{-\mathbf{q}y}^{\dagger} + H.c.) \\
& + J_{\parallel} \frac{(1-\lambda^2)^2}{(1+\lambda^2)^2} \sum_{\mathbf{q}} \gamma_{\mathbf{q}} (\tilde{z}_{\mathbf{q}}^{\dagger} \tilde{z}_{-\mathbf{q}}^{\dagger} + H.c.)
\end{aligned} \tag{17}$$

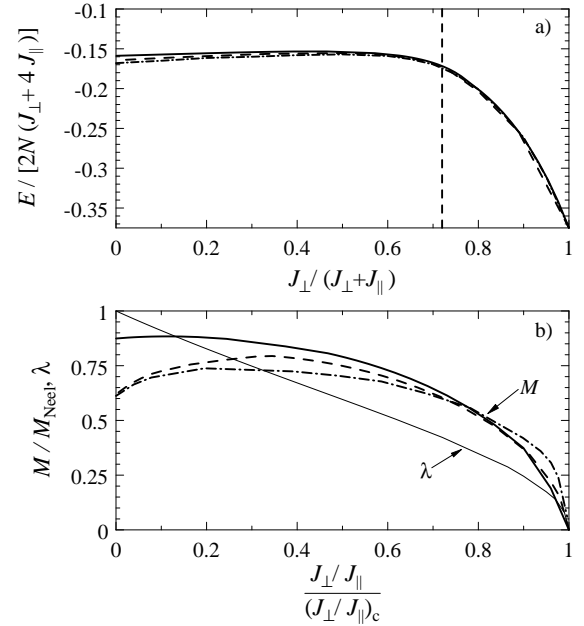


FIG. 1. a) Re-scaled ground-state energy E and b) staggered magnetization M for different approximation levels of the ground-state wave functions (11) and (13). Solid: Triplet pairs, no additional operators S_n , constraint exact, $(J_{\perp}/J_{\parallel})_c = 3.2$. Dashed: Triplet pairs, constraint ignored (spin-wave), $(J_{\perp}/J_{\parallel})_c = 4$. Dash-dot: Series expansion data taken from Ref. 6 for comparison, $(J_{\perp}/J_{\parallel})_c = 2.55$. The vertical dashed line in a) indicates the position of the magnetic quantum phase transition. In b) the coupling dependence of the basis parameter λ is also shown.

Another approximation we want to discuss briefly is to neglect the constraint (4) completely^{2,7} and also the quartic triplet terms in the Hamiltonians (6) and (10). The parameter λ is simply chosen so that the prefactors of the terms creating single \tilde{z} -bosons out of $|\tilde{\phi}_0\rangle$ vanish. One can formally set $\tilde{s} = 1$ (condensation of \tilde{s} -bosons); $|\tilde{\phi}_0\rangle$ can be considered as "vacuum". Neglecting the constraint (4) implies that the three types of excitations $\{\tilde{z}_i, t_{ix}, t_{iy}\}$ are treated as independent bosons. After a Fourier transformation one arrives at

with $\gamma_{\mathbf{q}} = \frac{1}{2}(\cos q_x + \cos q_y)$ and

$$\lambda = \sqrt{\frac{4J_{\parallel} - J_{\perp}}{4J_{\parallel} + J_{\perp}}} \quad (18)$$

in the ordered phase ($4J_{\parallel} > J_{\perp}$) and $\lambda = 0$ otherwise. The Hamiltonian (17) can be easily diagonalized by a Bogoliubov transformation. In this case the ground-state wave functions (11) and (13) (with pairs of triplet excitations) become exact. The described harmonic approximation can be considered as linear spin-wave theory for the bilayer problem **with** inclusion of longitudinal spin fluctuations². The critical coupling here becomes $(J_{\perp}/J_{\parallel})_c = 4$. In the limit of decoupled planes the results are equal to that of the linear spin-wave approach, e.g., the magnetization takes 60.5 % of its classical value, see Fig. 2. Further details on the ground-state calculations will be published elsewhere.

III. DESCRIPTION OF HOLE MOTION

If we remove one electron from rung i a single hole state on this rung is created. Let us denote by $a_{im,\sigma}^{\dagger}$ the creation operator of a hole with spin σ on rung i , where the index $m = 1, 2$ represents the number of the plane. This operator is defined by the equation

$$a_{im,\sigma}^{\dagger}|0\rangle = c_{i\bar{m},\sigma}^{\dagger}|0\rangle, \quad (19)$$

where $\bar{m} = 3 - m$. This is a fermionic operator which satisfies the usual anticommutation relations. The hole on the rung i interacts with the triplet excitations on its nearest-neighbor sites. The interaction Hamiltonian can be easily found by calculating all possible one-hole matrix elements of the initial Hamiltonian (1) (see Ref. 32). For the disordered phase ($\lambda = 0$) the result is

$$\begin{aligned} H_h = & -t_{\perp} \sum_{i\sigma} \left(a_{i1,\sigma}^{\dagger} a_{i2,\sigma} + H.c. \right) \\ & + \frac{t_{\parallel}}{2} \sum_{\langle ij \rangle m \sigma} \left(a_{im,\sigma}^{\dagger} a_{jm,\sigma} s_j^{\dagger} s_i + H.c. \right) \\ & + \frac{t_{\parallel}}{2} \sum_{\langle ij \rangle \sigma} \left(\mathbf{t}_i^{\dagger} \mathbf{t}_j a_{im,\sigma}^{\dagger} a_{jm,\sigma} + H.c. \right) \\ & + \sum_{\langle ij \rangle \sigma} \left(\mathbf{t}_i^{\dagger} \left[t_{\parallel} \mathbf{S}_{i,j} s_j + \frac{J_{\parallel}}{2} \mathbf{S}_{j,j} s_i \right] + H.c. \right) \\ & - t_{\parallel} \sum_{\langle ij \rangle} \left(i \bar{\mathbf{S}}_{j,i} \left[\mathbf{t}_i^{\dagger} \times \mathbf{t}_j \right] + H.c. \right) \\ & - \frac{J_{\parallel}}{2} \sum_{\langle ij \rangle} \left(i \bar{\mathbf{S}}_{i,i} \left[\mathbf{t}_j^{\dagger} \times \mathbf{t}_j \right] + H.c. \right). \quad (20) \end{aligned}$$

Following Refs. 32,36 we have introduced the notations $\mathbf{t} = (t_x, t_y, t_z)$ for the triplet vector and

$$\begin{aligned} \mathbf{S}_{i,j} &= \frac{1}{2} \sum_{m\alpha\beta} (-1)^m a_{im,\alpha}^{\dagger} \vec{\sigma}_{\alpha\beta} a_{jm,\beta}, \quad (21) \\ \bar{\mathbf{S}}_{i,j} &= \frac{1}{2} \sum_{m\alpha\beta} a_{im,\alpha}^{\dagger} \vec{\sigma}_{\alpha\beta} a_{jm,\beta}. \end{aligned}$$

for generalized hopping operators where $\vec{\sigma}$ is the vector of Pauli matrices. In addition we have to impose the constraint that a hole state and one of the doubly occupied states cannot coexist on the same rung:

$$s_i^{\dagger} s_i + \sum_{\alpha} t_{i\alpha}^{\dagger} t_{i\alpha} + \sum_{m\sigma} a_{im,\sigma}^{\dagger} a_{im,\sigma} = 1. \quad (22)$$

The several terms in the Hamiltonian (20) have been discussed by Eder³². They contain hopping without changing the spin background (direct hopping, second and third term) as well as spin-fluctuation assisted hopping (fourth and fifth term) and exchange processes where the hole remains on its rung (last two terms). Together with the Hamiltonian for the doubly occupied rungs (6) the Hamiltonian (20) contains the complete one-hole dynamics for the disordered phase. For the case of more than one hole additional hole interaction processes would have to be considered. However, in the present work we restrict ourselves to the discussion of the one-hole problem.

If we work in the magnetically ordered phase it is convenient to use the generalized basis $\{\tilde{s}, \tilde{z}, t_x, t_y\}$ from Sec. II to represent the states of the doubly occupied rungs. From the Hamiltonian (20) and the definition (8) of the basis operators one can construct a Hamiltonian for an ordered background state. It again contains processes proportional to t_{\parallel} where the hole hops to a neighboring rung and exchange terms proportional to J_{\parallel} . To be short we only state some hopping matrix elements of the resulting Hamiltonian. For that we symbolically introduce two-rung states $|XY\rangle = X_i^{\dagger} Y_j^{\dagger} |0\rangle$ where X and Y are the states on two adjacent rungs with $i \in A$ and $j \in B$.

$$\begin{aligned} \langle \tilde{s} a_{0\uparrow} | H_h | a_{0\uparrow} \tilde{s} \rangle &= \frac{t_{\parallel}}{2} \frac{1 - \lambda^2}{1 + \lambda^2}, \\ \langle \tilde{z} a_{0\uparrow} | H_h | a_{0\uparrow} \tilde{z} \rangle &= \frac{t_{\parallel}}{2} \frac{1 - \lambda^2}{1 + \lambda^2}, \\ \langle \tilde{z} a_{0\uparrow} | H_h | a_{0\uparrow} \tilde{s} \rangle &= -\frac{t_{\parallel}}{2} \frac{(1 + \lambda)^2}{1 + \lambda^2}, \\ \langle t_x a_{0\downarrow} | H_h | a_{0\uparrow} \tilde{s} \rangle &= -\frac{t_{\parallel}}{2} \frac{1 + \lambda}{\sqrt{1 + \lambda^2}}. \quad (23) \end{aligned}$$

The first two terms represent processes of hole motion without disturbing the spin background (so-called direct hopping) whereas the last two terms are examples for hole hopping with creation of a "spin defect". It can be seen that direct hopping is impossible in the limit of $|\lambda| = 1$, i.e., in a Néel-ordered background.

IV. SINGLE HOLE DYNAMICS

To investigate the hole motion we consider a one-particle Green's function describing the creation of a single hole with momentum \mathbf{k} at zero temperature:

$$G(\mathbf{k}, \omega) = \langle \psi_0 | \hat{c}_{\mathbf{k}\sigma}^\dagger \frac{1}{z-L} \hat{c}_{\mathbf{k}\sigma} | \psi_0 \rangle \quad (24)$$

where z is the complex frequency variable, $z = \omega + i\eta$, $\eta \rightarrow 0$. The quantity L denotes the Liouville operator defined by $LA = [H, A]_-$ for arbitrary operators A ; $\mathbf{k} = (k_x, k_y, k_z)$ is the hole momentum with $k_z = 0$ or π for the bonding or antibonding band, respectively. $|\psi_0\rangle$ is the full ground state of the undoped system as described in Sec. II. The effect of the hole creation operator $\hat{c}_{im,\sigma}$ applied to $|\psi_0\rangle$ can be related to the fermion operators $a_{im,\sigma}^\dagger$ introduced in the last section. One obtains for example for $i \in A$ sublattice

$$\begin{aligned} \hat{c}_{i1,\uparrow} \tilde{s}_i^\dagger |0\rangle &= \frac{1+\lambda}{\sqrt{2(1+\lambda^2)}} a_{i1,\downarrow}^\dagger |0\rangle, \\ \hat{c}_{i1,\uparrow} t_{ix}^\dagger |0\rangle &= -\frac{1}{\sqrt{2}} a_{i1,\uparrow}^\dagger |0\rangle, \end{aligned} \quad (25)$$

and analogous relations for other basis states and for $i \in B$.

The hole motion processes will be described in the concept of path operators^{18,19,23} which create strings of spin fluctuations attached to the hole. For the application of projection technique we define a set of path operators $\{A_I\}$ which couple to a hole and create local spin defects with respect to the undoped ground state $|\psi_0\rangle$. The first operator A_0 is the unity operator, the second one A_1 moves the hole by one lattice spacing creating one spin excitation and so on. We are interested in calculating dynamical correlation functions for the operators $\{A_I c_{\mathbf{k}\sigma}\}$:

$$G_{I\sigma, J\sigma'}(z) = \langle \psi_0 | (A_I c_{\mathbf{k}\sigma})^\dagger \frac{1}{z-L} (A_J c_{\mathbf{k}\sigma'}) | \psi_0 \rangle. \quad (26)$$

The Green's function (24) for the hole is then given by $G_{0\sigma, 0\sigma'}(z)$. Using cumulants the correlation functions G can be rewritten as²⁷:

$$G_{I\sigma, J\sigma'}(z) = \langle \phi_0 | \Omega^\dagger (A_I c_{\mathbf{k}\sigma})^\dagger \left(\frac{1}{z-L} A_J c_{\mathbf{k}\sigma'} \right) \Omega | \phi_0 \rangle^c. \quad (27)$$

The brackets $\langle \phi_0 | \dots | \phi_0 \rangle^c$ denote cumulant expectation values with $|\phi_0\rangle$. The "unperturbed" ground state at half-filling, i.e., one of the product states (5) or (9) for the disordered or ordered system, respectively, will be denoted in the following by $|\phi_0\rangle$ for both phases. The operator Ω has been described above, it transforms $|\phi_0\rangle$ being the ground state of H_0 into the full ground state $|\psi_0\rangle$ of $H = H_0 + H_1$ at half filling. In the following, Ω is approximated by an exponential ansatz as described in

Sec. II. Since the expression (27) contains both Ω and Ω^\dagger , the expectation values can be calculated only in the lowest non-trivial order of the fluctuations in Ω , i.e., the expansion will be restricted to linear fluctuation terms. In order to correctly describe the short-range spin fluctuations in the system, operators with up to 4 triplet excitations with a maximum distance of 4 lattice spacings have been employed. For the evaluation of their coefficients we have linearized the set of equations (12,14). This is possible since the absolute values of the coefficients are small compared to 1 as discussed in Sec. II C. Therefore quadratic and higher terms in the fluctuations operators can be neglected. By comparing the coefficients of the short-range fluctuations obtained in this way with the ones from the full (non-linear) ground-state calculation of Sec. II C we have numerically verified that the error in the matrix elements (30) introduced by this linearization is smaller than a few percent. Since the linearized equations for the coefficients do not yield a phase transition point we fix it at the value $(J_\perp/J_\parallel)_c = 2.55$ known from series expansions⁶ and Monte Carlo calculations³. (In the limit of an infinite set of operators $\{S_n\}$ within the cumulant method the solution of the non-linear equations has to yield the "exact" transition point which we assume to be at $(J_\perp/J_\parallel)_c = 2.55$.) In the ordered phase we set

$$\lambda = \sqrt{\frac{(J_\perp/J_\parallel)_c - J_\perp/J_\parallel}{(J_\perp/J_\parallel)_c + J_\perp/J_\parallel}} \quad (28)$$

which is suggested by the results obtained in Sec. II.

Using Mori-Zwanzig projection technique²⁸ one can derive a set of equations of motion for the dynamical correlation functions $G_{I\sigma, J\sigma'}(z)$. Neglecting the self-energy terms it reads:

$$\begin{aligned} \sum_{I\sigma} \Omega_{K\bar{\sigma}, I\sigma}(z) G_{I\sigma, J\sigma'}(z) &= \chi_{K\bar{\sigma}, J\sigma'}, \\ \Omega_{K\bar{\sigma}, J\sigma'}(z) &= z \delta_{KJ} \delta_{\bar{\sigma}\sigma'} - \sum_{L\sigma''} \omega_{K\bar{\sigma}, L\sigma''} \chi_{L\sigma'', J\sigma'}^{-1}. \end{aligned} \quad (29)$$

$\chi_{I\sigma, J\sigma'}$ and $\omega_{I\sigma, J\sigma'}$ are the static correlation functions and frequency terms, respectively. They are given by the following cumulant expressions:

$$\begin{aligned} \chi_{I\sigma, J\sigma'} &= \langle \phi_0 | \Omega^\dagger (A_I c_{\mathbf{k}\sigma})^\dagger (A_J c_{\mathbf{k}\sigma'}) \Omega | \phi_0 \rangle^c, \\ \omega_{I\sigma, J\sigma'} &= \langle \phi_0 | \Omega^\dagger (A_I c_{\mathbf{k}\sigma})^\dagger (L(A_J c_{\mathbf{k}\sigma'})) \Omega | \phi_0 \rangle^c. \end{aligned} \quad (30)$$

These terms describe all dynamic processes within the subspace of the Liouville space spanned by the operators $\{A_I c_{\mathbf{k}\sigma}\}$. The use of cumulants ensures size-consistency, i.e., only spin fluctuations connected with the hole enter the final expressions for the one-hole correlation function.

In the present calculations we have employed up to 1600 projection variables with a maximum path length of 3. The neglect of the self-energy terms leads to a discrete set of poles for the Green's functions, so the present approach cannot account for linewidths. In all figures we

have introduced an artificial linewidth of $0.2t_{\parallel}$ to plot the spectra. For details of the calculational procedure see e.g. Ref. 23.

A. One-hole spectrum

Now we turn to the discussion of the final results. First we consider the case of vanishing interplane hopping $t_{\perp} = 0$, i.e., the hole motion is restricted to one plane. (In this case k_z can be dropped.)

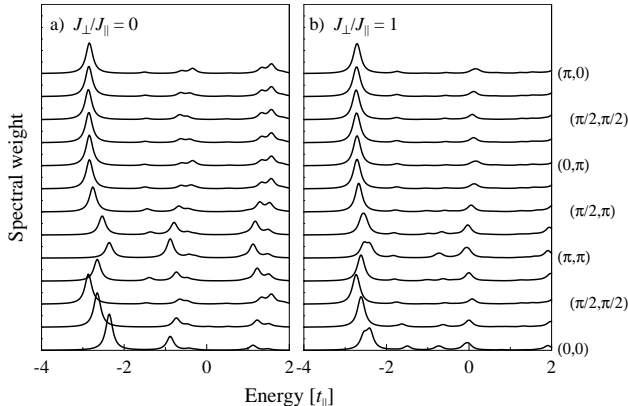


FIG. 2. One-hole spectral function for $t_{\perp} = 0$ (no interplane hopping), a) $J_{\perp}/J_{\parallel} = 0$, b) $J_{\perp}/J_{\parallel} = 1$, and different momenta (k_x, k_y) . The other parameters are $J_{\parallel}/t_{\parallel} = 0.4$; the energies are measured in units of t_{\parallel} relative to the energy of a localized hole.

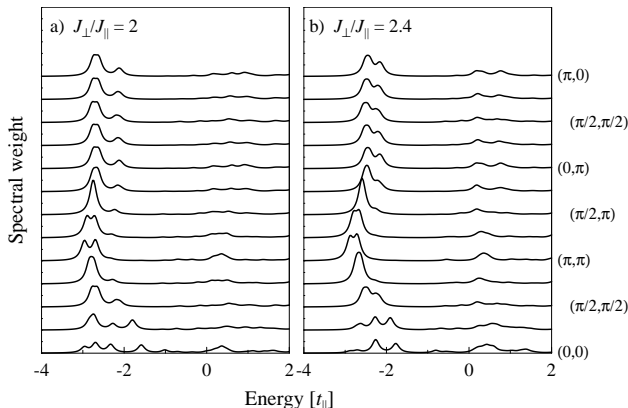


FIG. 3. Same as Fig. 2, but for a) $J_{\perp}/J_{\parallel} = 2$, b) $J_{\perp}/J_{\parallel} = 2.4$.

The one-hole spectral function $\text{Im} G(\mathbf{k}, \omega)$ for $t_{\perp} = 0$, $J_{\parallel}/t_{\parallel} = 0.4$ and various values of J_{\perp}/J_{\parallel} is shown in Figs. 2 - 4. For zero and small J_{\perp} , i.e., in the limit of decoupled planes, we observe a pronounced quasiparticle (QP) peak and a weak background at higher energies. The QP peak follows a dispersion with minima at $(\pm\pi/2, \pm\pi/2)$. These features are well-known from the one-hole problem in the single-layer antiferromagnet. With increasing J_{\perp}

the dispersion is "washed-out" because the antiferromagnetic correlations in the background state are weakened. At $J_{\perp}/J_{\parallel} \sim 1.5$ a cross-over to a dispersion with minima at (π, π) and $(0, 0)$ occurs. Note that this cross-over point still lies **inside** the antiferromagnet phase. Near the phase transition the spectral weight of the lowest pole at $(0, 0)$ becomes small. Most of the spectral weight can be found in a band with minimum at (π, π) and maximum at $(0, 0)$. The weak band visible at the bottom of the spectrum around momentum $(0, 0)$ can be considered as "shadow band" originating from the antiferromagnetic background, i.e., it is obtained by shifting the band with large weight by $\mathbf{Q} = (\pi, \pi)$.

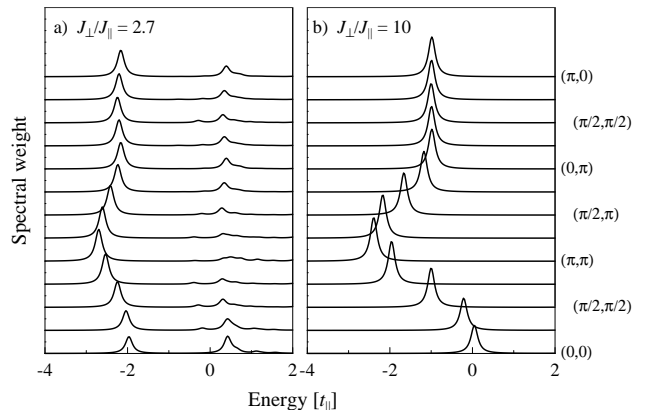


FIG. 4. Same as Fig. 2, but for a) $J_{\perp}/J_{\parallel} = 2.7$, b) $J_{\perp}/J_{\parallel} = 10$.

Further increasing J_{\perp} drives the system into the gapped paramagnetic (PM) phase. At the phase transition it can be seen that shadow bands being present in the AF phase disappear in the PM phase. At large J_{\perp} the hole behaves like a free fermion with a dispersion proportional to $t_{\parallel}(\cos k_x + \cos k_y)$.

Now we consider the effect of interplane hopping. We fix the ratio of the parameters to

$$\frac{t_{\perp}^2}{J_{\perp}} = \frac{t_{\parallel}^2}{J_{\parallel}} = \frac{U}{4} \quad (31)$$

which follows from the derivation of the $t - J$ model from a Hubbard model for the bilayer system with on-site repulsion U . Spectra for different parameter sets with $U/t_{\parallel} = 10$ are shown in Figs. 5 - 7. An interplane coupling of $t_{\perp}/t_{\parallel} = 1$ has already changed the character of the bands compared to $t_{\perp} = 0$ (cf. Fig. 2a). Further increasing t_{\perp}/t_{\parallel} to 1.5 (Fig. 6) forms a pronounced band with a free-fermion form at the bottom of the spectrum in the bonding channel ($k_z = 0$). In contrast, the antibonding spectrum ($k_z = \pi$) becomes incoherent since spectral weight is transferred to higher energies. Since we are still in the antiferromagnetic phase the lowest peaks in the antibonding channel appear at the same energies as in the bonding channel shifted by momentum $\mathbf{Q} = (\pi, \pi)$, i.e., these can again be considered as shadow bands. At

$t_{\perp}/t_{\parallel} > \sqrt{2.55}$ the AF order is destroyed. As shown in Fig. 7 for $t_{\perp}/t_{\parallel} = 2$ the shadow bands are disappeared, and in the antibonding channel a pronounced free-fermion band at high energies is formed. Higher values of t_{\perp} will completely suppress the incoherent weight left in the antibonding channel.

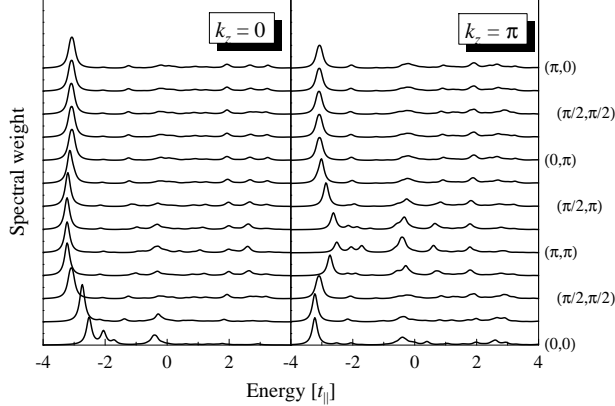


FIG. 5. One-hole spectral function for $t_{\perp}/t_{\parallel} = 1$, $J_{\perp}/J_{\parallel} = 1$, $J_{\parallel}/t_{\parallel} = 0.4$, and different momenta. The left and right panel show the bonding ($k_z = 0$) and antibonding ($k_z = \pi$) bands, respectively.

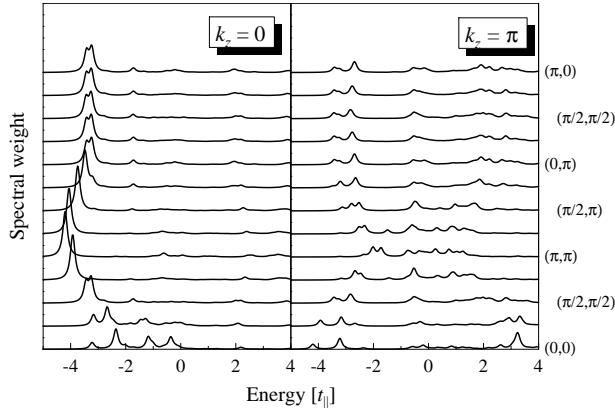


FIG. 6. Same as Fig. 5, but for $t_{\perp}/t_{\parallel} = 1.5$, $J_{\perp}/J_{\parallel} = 2.25$, and $J_{\parallel}/t_{\parallel} = 0.4$.

Varying the ratio $J_{\parallel}/t_{\parallel}$ (which is 0.4 for all figures presented here) does not change the picture qualitatively. Larger values of J_{\parallel} suppress the incoherent background in all spectra. For very small values of J_{\parallel} the spectral functions become incoherent since the hole is dressed with an increasing number of spin fluctuations, i.e., the radius of the spin polaron increases. Furthermore, the bandwidth of the quasiparticle dispersion at small J_{\perp} is mainly controlled by J_{\parallel} (instead of t_{\parallel}). This means that the bandwidth in units of t_{\parallel} decreases with decreasing $J_{\parallel}/t_{\parallel}$, see also next subsection. The location of the cross-over between the two dispersion forms depends weakly on $J_{\parallel}/t_{\parallel}$ which will be discussed below.

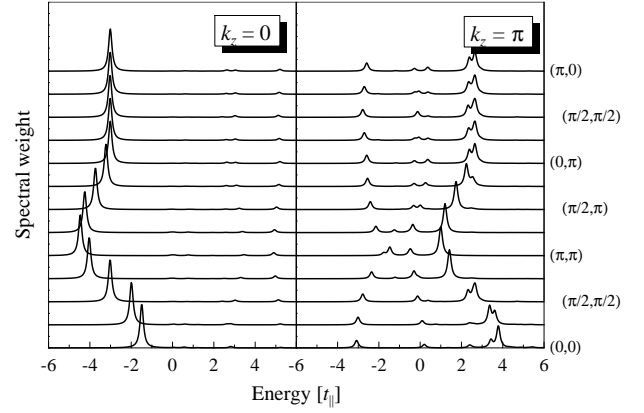


FIG. 7. Same as Fig. 5, but for $t_{\perp}/t_{\parallel} = 2$, $J_{\perp}/J_{\parallel} = 4$, and $J_{\parallel}/t_{\parallel} = 0.4$.

B. Quasiparticle bands

Next we are going to examine the properties of the low-lying bands. Again we first discuss the case of vanishing interplane hopping, $t_{\perp} = 0$. For $J_{\perp} \ll J_{\parallel}$ one finds a narrow QP band shown in Fig. 8 (top panel). It has minima at $(\pm\pi/2, \pm\pi/2)$ and a bandwidth of approximately $1.5J_{\parallel}$. It corresponds to the coherent motion of a dressed hole, i.e., a spin-bag quasiparticle. (Note that a larger set of path operators would give a larger bandwidth of around $2J_{\parallel}$ which is known from the calculations for a single-layer antiferromagnet²³. However, paths of length 4 and more are hard to access for the bilayer system due to the increasing numerical effort.)

The main contribution to the hole motion in the AF case can be understood as follows: the hopping hole locally destroys the antiferromagnetic spin order leaving behind a string of spin defects. Quantum spin fluctuations can repair pairs of frustrated spins which leads to a coherent motion in one of the antiferromagnetic sublattices (spin-fluctuation-assisted hopping). For $t_{\parallel}/J_{\parallel} > 1$ the bandwidth of this coherent hole motion is of order J_{\parallel} because the spin-flip part of the intraplane Heisenberg interaction J_{\parallel} is necessary to remove the spin defects caused by hopping.

With increasing J_{\perp} the bandwidth of the dispersion first decreases; at a value of $J_{\perp}/J_{\parallel} \sim 1.5$ the minima move to (π, π) and $(0, 0)$. Slightly larger values of J_{\perp} lead to an increase of the bandwidth, and spectral weight is transferred to a band which has nearly tight-binding form. So the lowest pole at $J_{\perp}/J_{\parallel} = 2.4$ has very small weight around momentum $(0, 0)$. This shadow band is shown as dashed line in Fig. 8. In the paramagnetic phase for larger J_{\perp} the shadow band disappears. The QP peak has a dispersion being nearly the one of a free fermion but with a reduced bandwidth. This behavior follows from the existence of the direct hopping term with prefactor $t_{\parallel}/2$ in H_h (20). It leads to a dispersion proportional to t_{\parallel} ; the saturation bandwidth equals half of the bandwidth of the uncorrelated system ($8t_{\parallel}$).

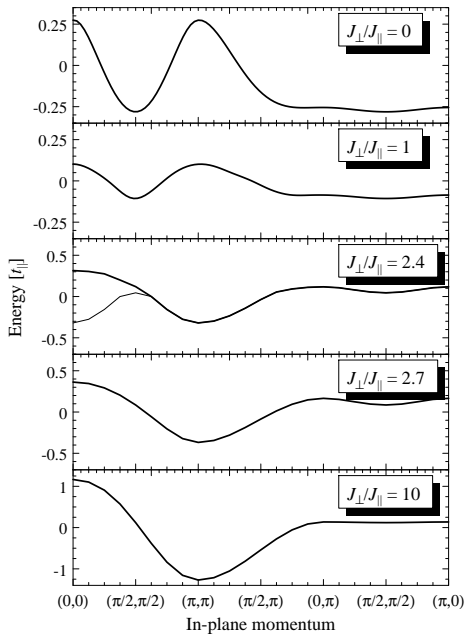


FIG. 8. Quasiparticle dispersion for $t_{\perp} = 0$ (no interplane hopping), $J_{\parallel}/t_{\parallel} = 0.4$, and different values of J_{\perp}/J_{\parallel} . The energy zero level has been set at the center of mass of the band. For $J_{\perp}/J_{\parallel} = 2.4$ the heavy line shows the dispersion of the peak carrying the main spectral weight whereas the thin line corresponds to the lowest pole in the spectrum (shadow band, see text).

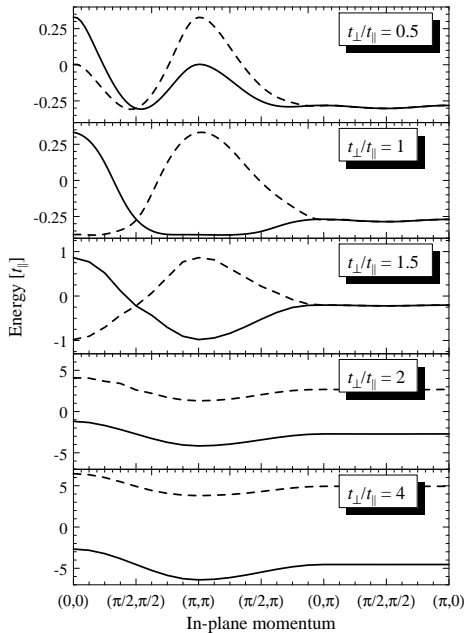


FIG. 9. Quasiparticle dispersion for $\frac{t_{\perp}^2}{J_{\perp}^2} = \frac{t_{\parallel}^2}{J_{\parallel}^2} = \frac{U}{4}$ with $U/t_{\parallel} = 10$ and different values of t_{\perp}/t_{\parallel} . The in-plane momentum (k_x, k_y) varies along the horizontal axis. Solid/dashed lines correspond to bonding/antibonding modes ($k_z = 0$ or π).

The results for non-zero interplane hopping t_{\perp} are

shown in Fig. 9. Again, for small t_{\perp} (small J_{\perp}) the dispersion character is "antiferromagnetic" whereas for large t_{\perp} (large J_{\perp}) the bands have a simple tight-binding form. For $J_{\perp} \gg J_{\parallel}$ and $t_{\perp} \gg t_{\parallel}$ their dispersion is given by

$$\epsilon_{\mathbf{k}} = -t_{\perp} \cos k_z + t_{\parallel} (\cos k_x + \cos k_y) \quad (32)$$

The bandwidth for the in-plane motion is reduced by a factor of 2 compared to a free fermion since the relevant hopping matrix element is $\langle sa_{0\uparrow} | H_h | a_{0\uparrow} s \rangle = t_{\parallel}/2$.

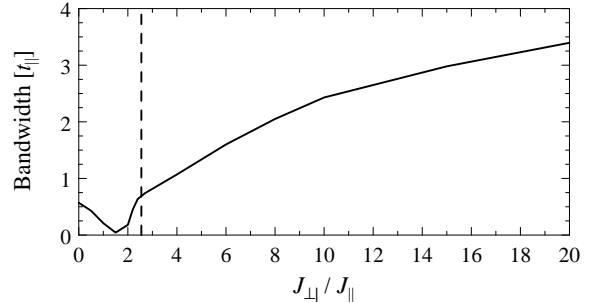


FIG. 10. Bandwidth of the quasiparticle dispersion (shown in Fig. 8) vs. J_{\perp}/J_{\parallel} for $t_{\perp} = 0$ (no interplane hopping) and $J_{\parallel}/t_{\parallel} = 0.4$. The vertical dashed line again indicates the position of the magnetic phase transition.

In Fig. 10 we finally show the bandwidth of the QP dispersion for the case of vanishing interplane hopping and $J_{\parallel}/t_{\parallel} = 0.4$, i.e., for the dispersions shown in Fig. 8. It can clearly be seen that the cross-over from an "antiferromagnetic" to a simple tight-binding dispersion occurs at $J_{\perp}/J_{\parallel} \sim 1.5$ and is connected with a pronounced minimum in the QP bandwidth. For $J_{\perp}/J_{\parallel} > 1.5$ the bandwidth increases and saturates for large J_{\perp} at $4t_{\parallel}$ as discussed above. Results for other values of $J_{\parallel}/t_{\parallel}$ are qualitatively similar. The minimum in the dispersion (i.e. the cross-over point) shifts with $J_{\parallel}/t_{\parallel}$: for $J_{\parallel}/t_{\parallel} = 0.1$ it is located at $J_{\perp}/J_{\parallel} \sim 1.1$, for $J_{\parallel}/t_{\parallel} = 10$ it is found at $J_{\perp}/J_{\parallel} \sim 2.0$. This in turn means that the cross-over in the shape of the single-hole dispersion can be driven by varying $J_{\parallel}/t_{\parallel}$ at fixed J_{\perp}/J_{\parallel} .

C. Relation to the short-range spin correlations

In order to understand the behavior of the QP dispersion and its bandwidth we illustrate in more detail the connection between the in-plane hole motion and the short-range in-plane spin correlations. The basic ingredient for the observed behavior of the QP dispersion is the competition between direct hopping which dominates in the disordered phase and spin-fluctuation-assisted hopping known from the single-layer AF. The relevant matrix element for direct hopping between states without spin deviations is $t_1 := \langle \psi_0 | \hat{c}_{j\sigma}^{\dagger} H_t \hat{c}_{i\sigma} | \psi_0 \rangle$ where

i, j are nearest-neighbor sites and $|\psi_0\rangle$ denotes the undoped background state. This term can be expressed^{23,35} by the static in-plane nearest-neighbor spin correlation $S_{\mathbf{R}} = \langle \psi_0 | \mathbf{S}_0 \cdot \mathbf{S}_{\mathbf{R}} | \psi_0 \rangle$ with $\mathbf{R} = (1, 0)$ as

$$t_1 = 2t_{\parallel} \left(S_{10} + \frac{1}{4} \right). \quad (33)$$

Spin-fluctuation-assisted hopping is more complicated since it involves two hopping steps and one spin-fluctuation process. The matrix element for the spin-fluctuation process (being the most important for not too small values of t_{\parallel}) can be written as $t_2 := \langle \psi_0 | \hat{c}_{j\sigma}^\dagger H_J A_2 \hat{c}_{i\sigma} | \psi_0 \rangle$ where A_2 moves the hole by two hopping steps (creating a path of spin defects) and i, j are now next-nearest neighbors. Transforming the expectation value into spin correlation functions one obtains^{23,35}

$$t_2 = J_{\parallel} \left(-\frac{1}{2} S_{10} + \frac{S_{20} + 2S_{11}}{4} + \frac{3}{16} \right) \quad (34)$$

where the average over the possible paths of length 2 has already been performed.

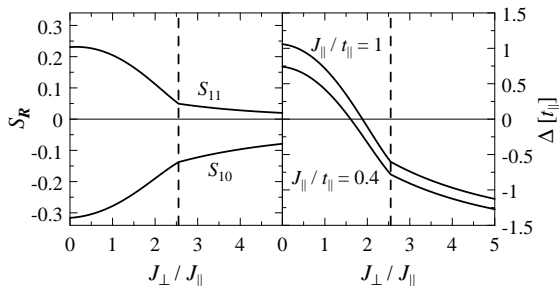


FIG. 11. Left: J_{\perp}/J_{\parallel} -dependence of the equal-time short-range spin correlation functions $S_{\mathbf{R}}$ in the spin background state calculated with the linearized exponential ansatz used for the description of the hole motion. Right: Δ vs. J_{\perp}/J_{\parallel} from eq. (35) for $J_{\parallel}/t_{\parallel} = 0.4$ and 1.0.

The in-plane dispersion shape can be described by the energy difference $\Delta = E(\pi, \pi) - E(\pi/2, \pi/2)$. Values $\Delta > 0$ correspond to an "antiferromagnetic" dispersion whereas $\Delta < 0$ occurs for a nearest-neighbor tight-binding dispersion. Neglecting longer paths and more complicated contributions to the hole motion the QP dispersion is given by the sum of a nearest-neighbor and a next-nearest neighbor dispersion originating from the two processes described above. Then Δ can be roughly estimated from the matrix elements t_1 and t_2 :

$$\Delta \sim -4t_1 + t_2. \quad (35)$$

The prefactor of t_1 arises from the number of nearest neighbors; for the t_2 -prefactor the influence of two hopping steps has to be kept in mind, a fit to numerical results for the single-layer problem yields a value of order 1. From this we see that the cross-over phenomenon can be

understood in terms of the interplay between short-range spin correlations and the ratio of J_{\perp}/t_{\parallel} .

Fig. 11 shows the values of $S_{\mathbf{R}}$ for nearest and next-nearest neighbor sites obtained from the present calculation. With increasing J_{\perp}/J_{\parallel} the absolute values of the in-plane spin correlation functions decrease from their single-layer values and are weakened within the antiferromagnetic phase. At the transition point the magnitude has dropped by a factor around 2–3 compared to $J_{\perp} = 0$ which again coincides with the fact that the density of spin (triplet) excitations is small in the disordered phase even at the transition point⁷. We have also plotted the quantity Δ estimated from eq. (35) for two different values of $J_{\parallel}/t_{\parallel}$. One notices a semi-quantitative agreement of the zero in Δ and the dispersion minimum described in Sec. IV B.

V. CONCLUSIONS

In this paper we have presented for the first time a systematic analytical study of the one-hole dynamics on both sides of a magnetic ordering transition in a low-dimensional antiferromagnet. The system under consideration was a bilayer antiferromagnet described by a t - J Hamiltonian in the limit of zero doping. The magnetic background state has been modelled with modified bond operators. In the disordered phase these operators describe the singlet ground state and the triplet excitations. In the AF ordered phase they account for the condensation of one type of triplet bosons and describe transverse as well as longitudinal fluctuations. Using the spin-polaron concept which describes the one-hole states in terms of local spin deviations we have calculated the one-hole spectral function for the whole range of magnetic couplings.

For the disordered background (large J_{\perp}/J_{\parallel} , gapped spin excitations) spin fluctuations around the hole are suppressed. The hole motion is dominated by direct hopping processes, i.e., hopping without disturbing the spin background. In the ordered phase for very small interplane coupling we recover the results known from the single-layer hole motion: The spectrum consists of a coherent QP peak at the bottom and an incoherent background. The QP can be associated with a mobile hole dressed by spin fluctuations. The bandwidth of its coherent motion is controlled by J_{\parallel} .

The cross-over between these two scenarios occurs **inside** the ordered phase where the antiferromagnetic short-range correlations become weakened. The cross-over is located between $1 < J_{\perp}/J_{\parallel} < 2$ depending on $J_{\parallel}/t_{\parallel}$ (for $J_{\parallel}/t_{\parallel} = 0.4$ it is found at $J_{\perp}/J_{\parallel} \sim 1.5$). Note that the cross-over can also be driven by variation of the hopping strength t_{\parallel} at a fixed value of J_{\perp}/J_{\parallel} well in the antiferromagnetic phase (e.g. 1.3). This behavior follows from the competition between direct nearest-neighbor hopping and spin-fluctuation-assisted

next-nearest-neighbor hopping. In contrast, when crossing the magnetic phase boundary at $J_{\perp}/J_{\parallel} \sim 2.5$ there are no drastic changes in the spectrum (and therefore in the ARPES response of such a system). The only differences between the spectra in both phases near the phase transition are weak shadow bands in some regions of the Brillouin zone in the AF phase.

Note that our approximation which describes the hole motion processes in terms of short-range spin fluctuations is questionable in a region in the close vicinity of the phase transition due to the existence of long-ranged critical fluctuations. However, it has been argued recently³⁶ that the influence of the critical modes suppresses the quasiparticle weight only in the limit of vanishing hopping $t/J \rightarrow 0$. In contrast, for finite hopping the number of spin fluctuations near the hole remains finite even at the transition point. So we expect the picture presented in this paper to be valid at least in the regions away from the transition, i.e., $|J_{\perp}/J_{\parallel} - 2.55| > 0.1$, which is supported by the fact that our spectral functions on both sides of the phase transition (e.g. at $J_{\perp}/J_{\parallel} = 2.4$ and 2.7) do not show major differences.

So the main result of the present paper can be summarized as follows: A magnetic phase transition has only weak influence on the ARPES spectrum of a doped antiferromagnet. The properties of the spectrum are, however, dominated by the short-range environment of the hole. The statement is expected to hold also for the doping-induced phase transition in the single-layer AF. Here the antiferromagnetic correlations are strong even in the paramagnetic phase, i.e., from the above considerations one expects to find an "antiferromagnetic" hole dispersion on both sides of the transition. This is exactly what was observed in recent work^{11,12}: analytical investigations of one hole in the AF phase as well as numerical studies of finite systems (which have a singlet ground state without long-range order) both show a coherent hole motion with a dispersion of width $2J$ and minima at $(\pm\pi/2, \pm\pi/2)$.

It should be pointed out that the above discussion applies to intermediate and high energy scales (order t, J) only. Of course there exist low-energy properties of the spectrum which are expected to be influenced by quantum criticality, e.g., the linewidth in a finite-temperature photoemission experiment should show scaling behavior in the quantum-critical region associated with the transition³⁷. These features as well as the hole dynamics in the bilayer system at low but finite doping are beyond the scope of the present study and will be subject of future research.

ACKNOWLEDGMENTS

The authors thank E. Dagotto and T. Sommer for useful conversations. M.V. acknowledges support by the DFG (VO 794/1-1).

-
- ¹ Y. Uemura, Phys. Rev. Lett. **66**, 2665 (1991), T. Imai *et al.*, Phys. Rev. Lett. **70**, 1002 (1993), M. Takigawa, Phys. Rev. B **49**, 4158 (1994), G. Aeppli, T. E. Mason, S. M. Hayden, H. A. Mook, and J. Kulda, Science **278**, 1432 (1997).
 - ² A. V. Chubukov and D. K. Morr, Phys. Rev. B **52**, 3521 (1995).
 - ³ A. W. Sandvik and D. J. Scalapino, Phys. Rev. Lett. **72**, 2777 (1994).
 - ⁴ A. W. Sandvik, A. V. Chubukov, and S. Sachdev, Phys. Rev. B **51**, 16483 (1995).
 - ⁵ C. N. A. van Duin and J. Zaanen, Phys. Rev. Lett. **78**, 3019 (1997).
 - ⁶ W. H. Zheng, Phys. Rev. B **55**, 12267 (1997).
 - ⁷ V. N. Kotov, O. P. Sushkov, W. H. Zheng, and J. Oitmaa, Phys. Rev. Lett. **80**, 5790 (1998).
 - ⁸ K. Hida, J. Phys. Soc. Jpn. **59**, 2230 (1990).
 - ⁹ A. J. Millis and H. Monien, Phys. Rev. Lett. **70**, 2810 (1993), Phys. Rev. B **50**, 16606 (1994).
 - ¹⁰ Y. Matsushita, M. P. Gelfand, and C. Ishii, J. Phys. Soc. Jpn. **68**, 247 (1999), D.-K. Yu, Q. Gu, H.-T. Wang, and J.-L. Shen, Phys. Rev. B **59**, 111 (1999).
 - ¹¹ E. Dagotto, Rev. Mod. Phys. **66**, 763 (1994).
 - ¹² W. Brenig, Phys. Rep. **251** 153 (1995).
 - ¹³ J. Igarashi and P. Fulde, Phys. Rev. B **45**, 12357 (1992), G. Khaliullin and P. Horsch, Phys. Rev. B **47**, 463 (1993), A. Belkasri and J. L. Richard, Phys. Rev. B **50**, 12896 (1994).
 - ¹⁴ M. Vojta and K. W. Becker, Ann. Phys. (Leipzig) **5**, 156 (1996), Phys. Rev. B **54**, 15483 (1996).
 - ¹⁵ B. O. Wells *et al.*, Phys. Rev. Lett. **74**, 964 (1995).
 - ¹⁶ D. S. Dessau *et al.*, Phys. Rev. Lett. **71**, 2781 (1993).
 - ¹⁷ D. S. Marshall *et al.*, Phys. Rev. Lett. **76**, 4841 (1996).
 - ¹⁸ Y. Nagaoka, Phys. Rev. **147**, 392 (1966), W. F. Brinkman and T. M. Rice, Phys. Rev. B **2**, 1324 (1970), B. I. Shraiman and E. D. Siggia, Phys. Rev. Lett. **60**, 740 (1988).
 - ¹⁹ S. A. Trugman, Phys. Rev. B **37**, 1597 (1988).
 - ²⁰ J. R. Schrieffer, X. G. Wen, and S. C. Zhang, Phys. Rev. Lett. **60**, 944 (1988), E. Dagotto and J. R. Schrieffer, Phys. Rev. B **43**, 8705 (1991).
 - ²¹ G. Martinez and P. Horsch, Phys. Rev. B **44**, 317 (1991).
 - ²² J. A. Riera and E. Dagotto, Phys. Rev. B **55**, 14543 (1997).
 - ²³ M. Vojta and K. W. Becker, Phys. Rev. B **57**, 3099 (1998).
 - ²⁴ A. Nazarenko and E. Dagotto, Phys. Rev. B **54**, 13058 (1996), W.-G. Yin and C.-D. Gong, Phys. Rev. B **56**, 2843 (1997).
 - ²⁵ R. Eder, Y. Ohta, and S. Maekawa, Phys. Rev. B **51**, 3265 (1995), Phys. Rev. B **52**, 7708 (1995).
 - ²⁶ K. W. Becker and P. Fulde, Z. Phys. B **72**, 423 (1988).
 - ²⁷ K. W. Becker and W. Brenig, Z. Phys. B **79**, 195 (1990).
 - ²⁸ H. Mori, Progr. Theor. Phys. **34**, 423 (1965), R. Zwanzig, in: Lectures in Theoretical Physics vol. 3. New York: Interscience 1961.
 - ²⁹ T. Schork and P. Fulde, J. Chem. Phys. **97**, 9195 (1992).
 - ³⁰ S. Sachdev and R. N. Bhatt, Phys. Rev. B **41**, 9323 (1990).

- ³¹ S. Gopalan, T. M. Rice, and M. Sigrist, Phys. Rev. B **49**, 8901 (1994).
- ³² R. Eder, Phys. Rev. B **57**, 12832 (1998).
- ³³ K. Kladko and P. Fulde, Int. J. Quant. Chem. **66**, 377 (1998).
- ³⁴ R. F. Bishop, Theor. Chim. Acta **80**, 95 (1991), R. F. Bishop, R. G. Hale, and Y. Xian, Phys. Rev. Lett. **73**, 3157 (1994), C. Zeng, D. J. J. Farnell, and R. F. Bishop, J. Stat. Phys. **90**, 327 (1998).
- ³⁵ Y. Takahashi, Z. Phys. B **71**, 425 (1988), R. Hayn, J. L. Richard, V. Yu. Yushankhai, Solid State Comm. **93**, 127 (1995).
- ³⁶ O. P. Sushkov, unpublished.
- ³⁷ T. Valla, A. V. Fedorov, P. D. Johnson, B. O. Wells, S. L. Hulbert, Q. Li, G. D. Gu, and N. Koshizuka, Brookhaven preprint (1999).